Biodegradation assessment of PLA and its nanocomposites

A. Araújo • M. Oliveira • R. Oliveira • G. Botelho • A. V. Machado

Abstract

Poly(lactic acid) nanocomposites containing Cloisite 15A, Cloisite 30B, and Dellite 43B were prepared by melt-mixing in a batch mixer and were exposed to UV radiation, temperature, and microorganism in solution and in a compost. Exposed samples, collected along the time, were characterized by several techniques. While the addition of organoclays had a positive effect on thermal stability, the degradation rate of nanocomposites increased when exposed to UV radiation and microorganism. Moreover, the degradation rate depends on the organoclay type. Even though the degradation rate is higher for nanocomposites, Fourier transform infrared spectrometry and gel permeation chromatography results demonstrated that the degradation mechanism is the same.

Keywords PLA • Nanocomposites • Biodegradation • Degradation · Compost · Environment

Introduction

Recently, much attention has been paid to biodegradable polymers due to their wide range of applications in packaging, agriculture, or biomedical fields and due to the increase of social concerns about waste pollution. Poly(lactic acid) (PLA), a linear thermoplastic polyester produced by the ring opening polymerization of lactide, is one of the most important and widely studied biodegradable polymers. It can be produced

from renewable resources at low cost, is recyclable to its monomers, and is a potential substitute to petroleum-based polymers (Carrasco et al. 2010; Dadbin et al. 2011).

The main limitations of PLA towards wider industrial application are poor thermal and mechanical resistance and limited gas barrier properties, which limit the access to some industrial sectors (Fukushima et al. 2009b). Nevertheless, published investigations have shown that these properties can be enhanced by the addition of low amounts of nanoclays, mainly organic modified montmorillonite (MMT) (Zhu et al. 2011; Wu and Wu 2006; Wu et al. 2009; Lewitus et al. 2006; Fukushima et al. 2013) without eco-toxicity (Bikiaris 2011; Bordes et al. 2009).

According to published data, PLA degradation depends on several parameters, such as molecular weight, crystallinity, purity, temperature, pH , presence of terminal carboxyl or hydroxyl groups, water permeability, and additives acting catalytically (Zhou and Xanthos 2009; Carrasco et al. 2010). Thermal degradation of PLA can occur by several mechanisms, such as hydrolysis by trace amounts of water and oxidative random main-chain scission, resulting in the formation of monomer and oligomer lactides of low

molecular weight (Madhavan Nampoothiri et al. 2010). Recently, a new photooxidation mechanism of PLA based on the formation of an anhydride was proposed (Gardette et al. 2011; Bocchini et al. 2010; Frache and Bocchini 2013). This mechanism involves a classical hydrogen abstraction on the polymeric backbone at the tertiary carbon in the α-position of the ester function leading to macroradical formation. It is postulated that initiation of the photochemical reaction results from the presence of chromophoric defects in the polymer at very low concentrations (Therias et al. 2012). This mechanism contradicts the older mechanism reported in the literature, which is associated with a Norrish II-type photo-cleavage (Belbachir et al. 2010; Ikada 1997).

The study of degradation and biodegradation of biodegradable polymer nanocomposites using laboratory-scale test methods is an extremely important area from scientific and industrial point of view, providing knowledge to predict these materials behavior after disposal (Copinet et al. 2003; Zaidi et al. 2010b).

There are several methods currently available to assess the biodegradability of polymer materials (Pagga 1997). In general, they are based on an indirect measurement, such as oxygen consumption, carbon dioxide production, or biogas generation (Massardier-Nageotte et al. 2006).

Biodegradation of PLA has been studied and reported, and it depends mainly on its molecular weight and on the environmental conditions to which it is exposed (Petinakis et al. 2010). Upon disposal in the environment, it is hydrolysed into low-molecular-weight oligomers and then mineralized into CO_2 and H_2O by the microorganisms present in the environment (Tokiwa and Calabia 2006).

The effect of nanoparticles on the biodegradation of PLA has attracted great interest recently. Some authors studied the effect of nanoclay on the biodegradation and found out that the clay accelerated the polymer biodegradation (Fukushima et al. 2009a; Sinha Ray et al. 2003b). However, other studies reported that nanoclays can be able to retard the degradation of aliphatic polyesters during biodegradation, attributing this effect to the enhanced barrier properties of the layered silicate nanocomposites (Lee et al. 2002; Rhim et al. 2013).

Therefore, this study aims to evaluate the degradability and biodegradability of PLA and its nanocomposites using different approaches. Nanocomposites with three different nanoclays (Cloisite 30B, Cloisite 15A, and Dellite 43B) were prepared by melt-mixing and exposed to UV radiation, temperature, and microorganisms (solution and compost). Samples were removed along the time and characterized by several techniques.

Materials and methods

Materials

A commercial PLA grade (3251D) was supplied by NatureWorks LLC (USA). The three nanoclays (modified MMT) used were supplied by Southern Clay Products (USA), Cloisite 30B (C30B) and Cloisite 15A (C15A), and by Laviosa Mineraria (Italy), Dellite 43B (D43B),

respectively. Tetrahydrofuran (THF) (99.9 %) was purchased from Riedel-de Haën and used without further treatment.

Sample preparation

Nanocomposites were prepared by melt-mixing according to the following procedure. PLA pellets and nanoclays were dried in a vacuum oven at 60°C for 12 h . PLA with 3wt. % of C15A, C30B, and D43B were pre-mixed and introduced in a Haake batch mixer (HAAKE Rheomix 600 OS; volume 69 cm^3) equipped with two rotors running in a counterrotating way. The set temperature was 190°C, and the rotor speed was 80 rpm . After 5 min of mixing time, the total sample was removed.

For degradation studies, the prepared nanocomposites were pressed into thin films by compression molding at 200 °C under 30 ton for 60 s . The thickness of each film (ca. 40μ m) was measured with a pachymeter Mitutoyo.

Thermo- and photo-oxidative degradation

Thermo-oxidative degradation experiments were carried out in an oven under air at 140°C along 120 h using rectangular thin films of PLA and nanocomposites.

The accelerated weathering of PLA and nanocomposites were carried out in a XenoTest 150 S chamber from Heraeus (Original Hanau) equipped with a filtered Xenon lamp with an intensity of 60Wm^{-2} according to standard procedures (ISO-4892-2 2006). The light of the xenon lamp was filtered under 300 nm with an UV window combined with six IR filter glasses. PLA and nanocomposites with dimensions of 135 × 45 mm were cut from the thin films. Samples were removed after 100,200,300,400,500, and 600 h of exposure and characterized.

Biochemical oxygen demand test

Biodegradation of PLA and nanocomposites (powder form) was assessed in aqueous environment under aerobic conditions according to standard procedure (ISO-14851 1999 (withdrawn 2005)), which specify a method for the determination of biochemical oxygen demand in a closed respirometer, as described in Moura et al. (2011).

Composting

Biodegradation in compost was performed on compression molded (25 × 25 × 0.125 mm) samples at 40°C. Samples were placed in compost made of soil and activated sludges from waste water treatment, keeping a relative humidity of approximately 50 – 70%. Around 20 samples of each material were vertically buried at 4 – 6 cm depth to guarantee aerobic degradation conditions at a horizontal distance of 5 – 6 cm between samples. At selected times (every 3 weeks), samples were collected, washed with water, and dried at room temperature until constant weight was reached. Based on the sample weight before and

after composting, the average percentage of residual mass for each material was calculated.

Characterization

Mechanical properties

The mechanical properties of PLA and nanocomposites were characterized using stress-strain experiments in a Zwick Rowell equipment. The tensile experiments were carried out with a deformation rate of 50 mm/min at room temperature under a relative humidity of 50%. The tests were performed on 8×0.6 cm rectangular samples in a longitudinal direction. At least 12 specimens of each sample were tested.

Scanning electron microscopy
Scanning electron microscopy (SEM) analysis was performed in a Leica Cambridge S360 microscope. Samples were previously fractured in liquid nitrogen and coated with a thin gold film.

Fourier transform infrared spectroscopy

Room temperature infrared spectra of the initial and degraded samples were recorded on an ABB FTLA 2000 spectrometer in the range $4{,}000 - 500\ \mathrm{cm}^{-1}$ by averaging 16 scans and using a resolution of $4\ \mathrm{cm}^{-1}$.

Viscosimetry

The intrinsic viscosity (η) of all samples (initial and degraded) was determined using an Ubbelohde capillary viscometer, with $5\mathrm{mgmL}^{-1}$ solutions in chloroform at $25.0 \pm 0.5°\mathrm{C}$ and according to the following equation (Zhou and Xanthos 2009):

$$\eta = \frac{\sqrt{2\left((\eta_r - 1) - \ln\ \eta_r\right)}}{c}$$

where η_r is relative viscosity and c is polymer solution concentration.

Five measurements were performed and averaged to obtain the solution viscosity of each sample.

Gel permeation chromatography

Gel permeation chromatography (GPC) was used to determine the molecular weight distribution of the PLA and nanocomposites before and after biodegradation. Solutions were prepared in THF and prefiltered on filter disk (hydrophobic polytetrafluoroethylene, 0.45μ m pore size) before injection. A Waters Alliance GPC Model 2695, equipped with three PLgel MIXED-B columns (inner diameter = 7.5 mm, length = 30 mm, and particle size = 10μ m). THF was used as eluent with a flow rate of 1 mL/ min , and the temperatures were 25 and $35°\mathrm{C}$ at the injector and detector, respectively.

Results and discussion

The mechanical properties of PLA and nanocomposites are shown in Fig. 1. It can be found that the tensile strength of the nanocomposites decreased when compared with PLA. This might be due to the absence of strong interaction between PLA matrix and nanoclay layers, which resulted in lots of cavities that appeared at lower tensile stress and a subsequent premature yielding (Li et al. 2009). The higher decrease was observed for nanocomposites with C15A probably because of the presence of clay agglomerates as depicted in SEM pictures (Fig. 2). An increase of tensile modulus was achieved for all nanocomposites. The enhancement of the tensile modulus of nanocomposites can be attributed to the clay layer rigidity and the higher crystallinity degree of the nanocomposites (Li et al. 2009). Nanocomposites with C30B and D43B present higher modulus due to its better dispersion and intercalated structure (Araújo et al. 2013). As anticipated, the elongation at break decreased for PLA nanocomposites, and according to Zaidi et al., the results are related to the weak interaction between the polymer and the clays layers (Zaidi et al. 2010a).

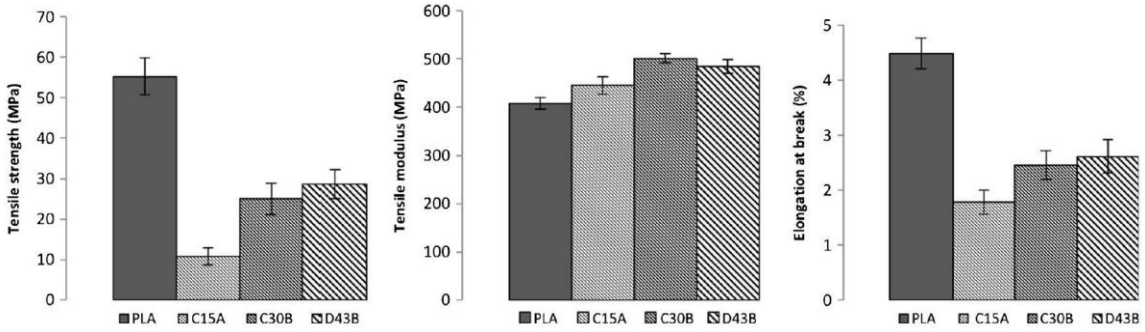

Fig. 1 Tensile strength (megapascals), tensile modulus (megapascals), and elongation at break (percent) for PLA and nanocomposites

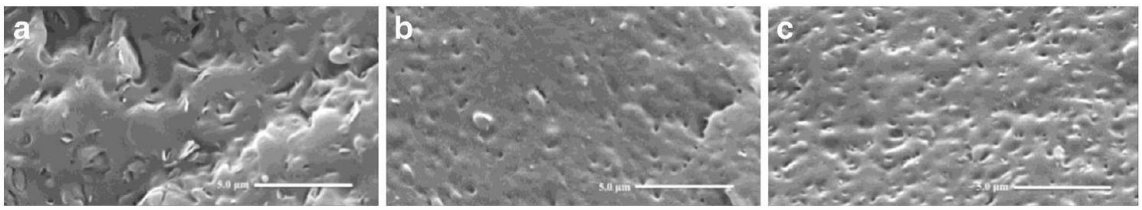

Fig. 2 SEM pictures of PLA with a C15A, b C30B, and c D43B

Fourier transform infrared (FTIR) spectra of PLA and nanocomposites with 3wt% nanoclays incorporation were obtained before and after 120 h of thermal degradation and after 600 h of photodegradation. Figures 3 and 4 presents the spectra obtained for nanocomposites containing the organoclay C30B and D43B, respectively.

After thermal degradation, some changes can be detected, including the increase and the decrease of characteristics bands (Araújo et al. 2013). Two new shoulders appeared at 1,724 and 1,714 cm^{-1} after degradation for all nanocomposites, and these can be associated to the formation of new carbonyl compounds. Also, a decrease at 955 cm^{-1} can be seen corresponding to the presence of an amorphous region (Meaurio et al. 2006) and

the appearance of the new band at 920 cm^{-1}, characteristic of α crystals (Kister et al. 1998; Liu et al. 2006).

After photodegradation, higher band intensity can be detected for nanocomposites, enlargement of the band corresponding to $C = O$, and the appearance of a shoulder at 1,845 cm^{-1} more intense for nanocomposites with C30B. According to literature data, this band is assigned to anhydride groups (Bocchini et al. 2010; Gardette et al. 2011) and is in agreement with the photo-degradation mechanism proposed by Bocchini et al. (2010) and Gardette et al. (2011).

The overall FTIR spectra present in Figs. 3 and 4 are quite similar to the one obtained for PLA and for PLA with C15A; no vibration modes are totally suppressed; no new modes seem to appear due to nanoclays presence, and therefore, any changes on PLA structure are due to degradation and not due to nanoclays addition. Even though the degradation rate under UV radiation was higher for nanocomposites than for PLA, the photodegradation mechanism was not affected by the nanoclays presence.

Intrinsic viscosity (η) measurements were performed for initial and samples exposed to temperature and UV radiation, and results are presented in Fig. 5. Before exposure, all nanocomposites exhibited lower viscosity than PLA; this decrease can be related with chain scission that occurred during its preparation, due to high temperature, shear during melt mixing, and reactions between PLA and reactive groups of the clay modifiers (Zhou and Xanthos 2009; Zaidi et al. 2010b). A very high sensitivity of PLA to thermal degradation during melt processing has been reported even in the presence of an antioxidant (Pandey et al. 2005).

According to the results of Fig. 5, the incorporation of nanoclays into PLA decreased the PLA UV stability after

600 h . The PLA nanocomposites degraded faster than pristine PLA as a consequence of the oxidation induction time (OIT) reduction (Frache and Bocchini 2013). Several hypotheses were proposed to explain the OIT reduction: adsorption of antioxidants onto the nanofiller, catalytic effect of transition metal impurities of nanofiller, and degradation of the alkyl ammonium cations of MMT (Bocchini et al. 2010; Zaidi et al. 2010a). The catalytic effect of MMT, as described by Bocchini, is due to the presence of transition metals on its surface that rapidly decomposed inducing a higher oxidation rate (Bocchini et al. 2010). Metal ions can catalyze the oxidation of polymers by several processes, including the decomposition of hydroperoxides, accelerating the whole degradation process (Bocchini et al. 2010; Frache and Bocchini 2013). The photooxidation was higher for nanocomposites prepared with C30B and C15A, and according to our previous work, the degradation rate of these nanocomposites was similar (Araújo et al. 2013). A possible explanation for higher chain scission in the sample containing C30B is the presence of hydroxyl groups in its chemical structure that could promote the hydrolysis of PLA macromolecules (Solarski et al. 2008), and this result is supported by FTIR (Fig. 3), in which the shoulder at 1, 845 cm^{-1}, assigned to anhydride groups, was more intense. The high decrease in viscosity of the nanocomposite containing C15A was not expected, since this nanoclay does not present reactive functional groups. Therefore, this decrease can be initial molecular weight of the nanocomposites or the presence of clay aggregates can absorb water, which could promote hydrolysis of the PLA chains.

After 120 h of thermal exposure, PLA and nanocomposites exhibit a decrease in viscosity. This decrease was lower for nanocomposites than for PLA. This behavior is explained by

the capability of clays to adsorbed and weaken the acid sites responsible by polymer degradation (Okamoto et al. 2005). Moreover, when a good dispersion of nanofillers is achieved, it acts as strong barrier, retarding the degradation process. During thermal oxidation, organic modifiers start to decompose, forming a carbonaceous-silicate char structure (Fig. 6). Once formed, it acts as isolator and mass transfer barrier, delaying the diffusion of oxygen, reducing the degradation (Zhou and Xanthos 2009). Thus, the incorporation of nanoclays enhances the PLA thermal stability. Nanocomposites with D43B presented higher thermal stability, and this was expected since D 43 B do not have reactive chemical groups that could induce PLA chain scission.

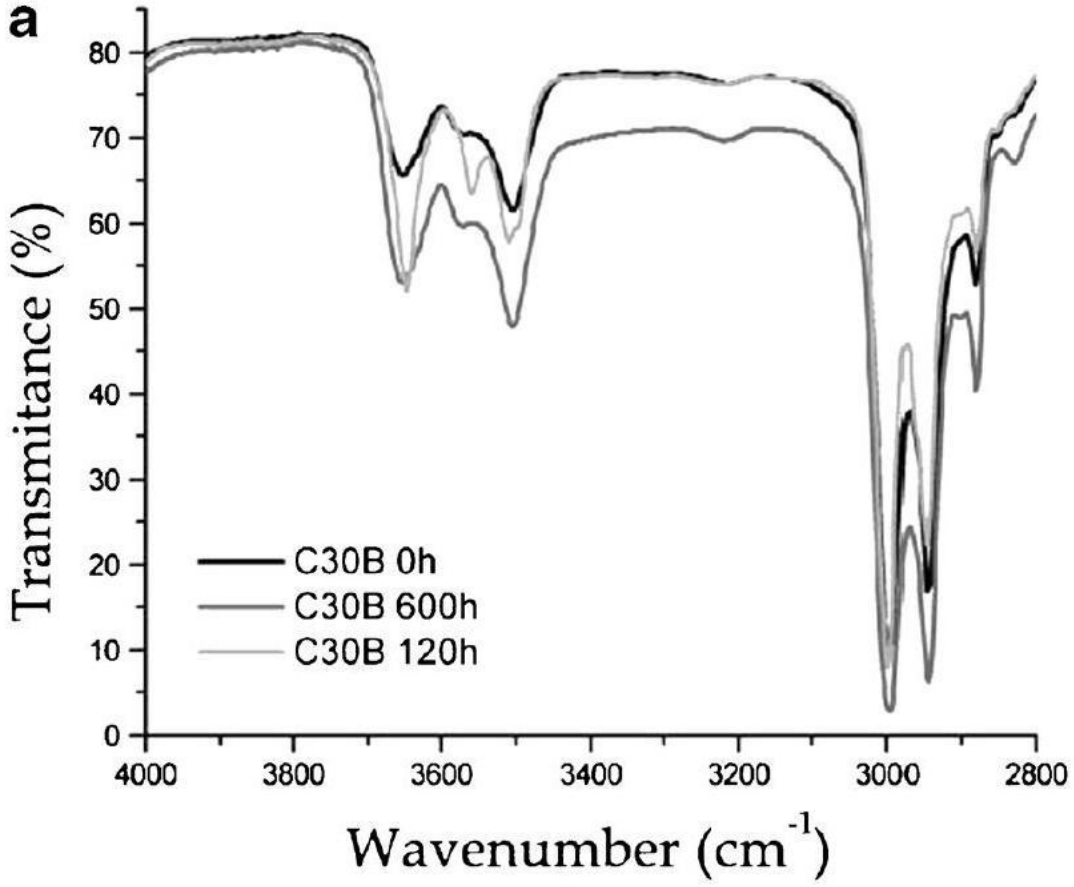
a
Transmitance (%)
Wavenumber (cm-1)
C30B 0h
C30B 600h
C30B 120h
b
Transmitance (%)
Wavenumber (cm-1)
C30B 0h
C30B 600h
C30B 120h

Fig. 3 FTIR spectra of PLA with C30B before and after 120 h of thermal degradation and 600 h of photodegradation in three regions: a 4,0002,800 , b 2,000 – 1,500 and c 1,500 – 500 cm^{-1}

The biodegradability of PLA and nanocomposites was determined by biochemical oxygen demand in a closed

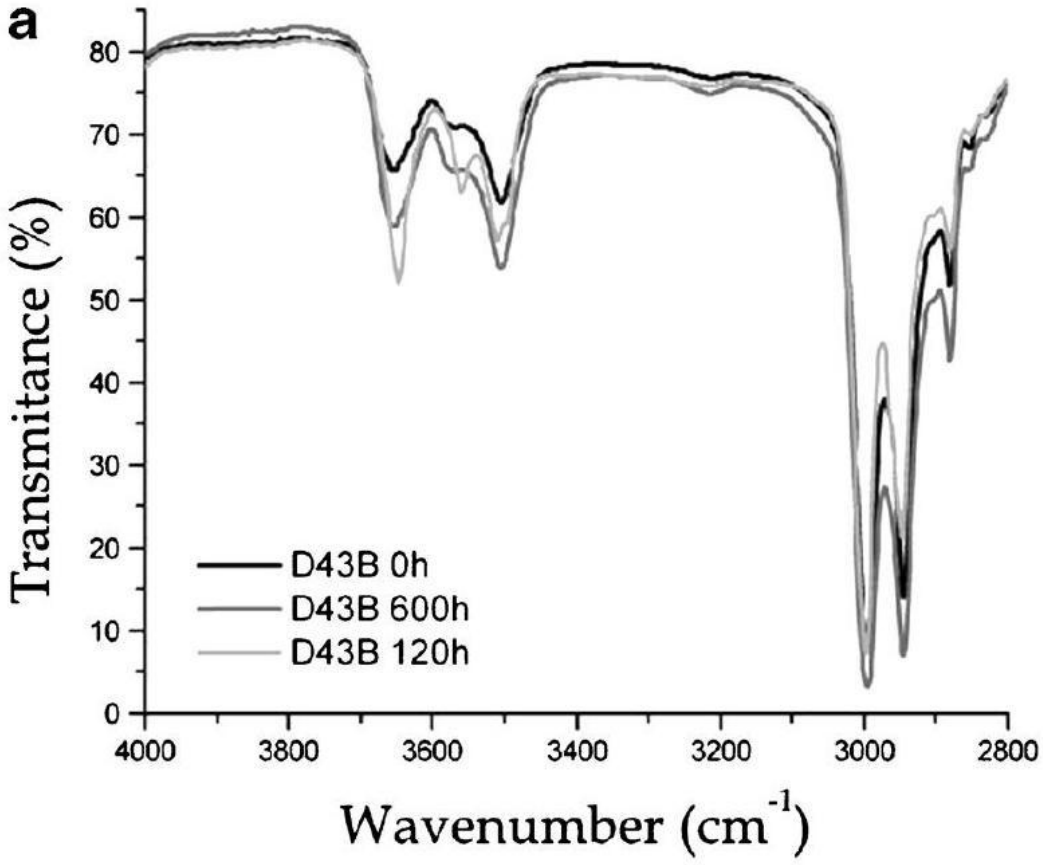
a
Transmitance (%)
Wavenumber (cm-1)
D43B 0h
D43B 600h
D43B 120h
4000
3800
3600
3400
3200
3000
2800

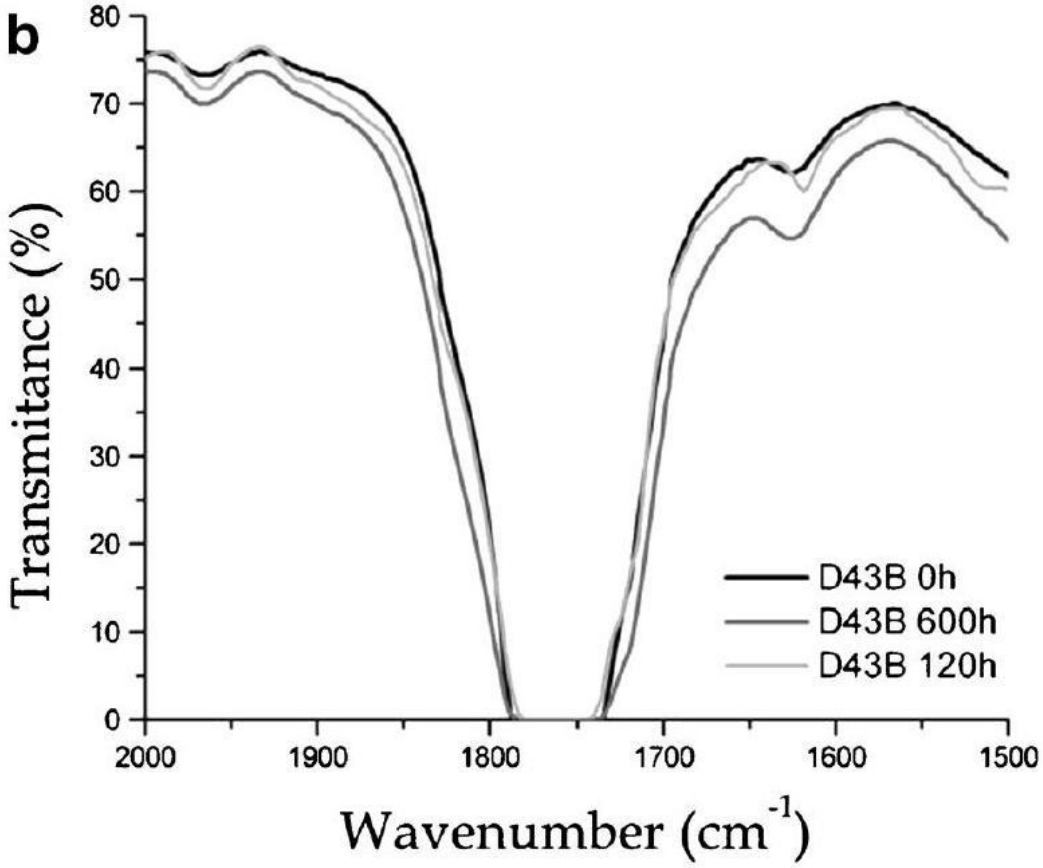
b
Transmitance (%)
Wavenumber (cm-1)
D43B 0h
D43B 600h
D43B 120h
2000
1900
1800
1700
1600
1500


c

Fig. 4 FTIR spectra of PLA with D43B before and after 120 h of thermal degradation and 600 h of photodegradation in three regions: a 4,0002,800 , b 2,000 – 1,500, and c 1,500 – 500 cm^{-1}

respirometer (ISO-14851 1999 (withdrawn 2005)) during 35 days (when a plateau of oxygen consumption was achieved). The values were expressed as the amount of O_2

Fig. 5 Intrinsic viscosity for initial and degraded samples

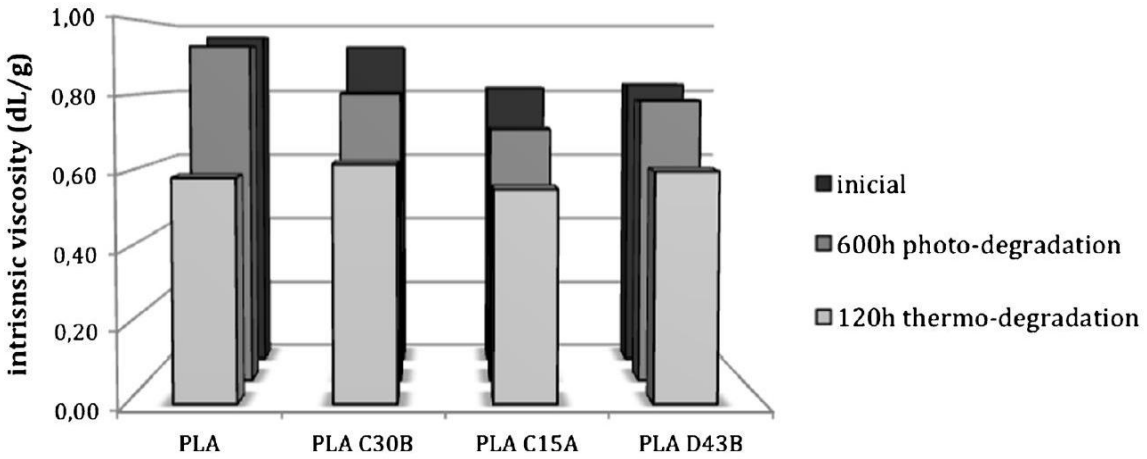

consumed during sample biodegradation divided by their theoretical oxygen demand and are presented in Fig. 7. The experimental results show that the biodegradability of PLA and nanocomposites is similar in the first days. After 35 days, PLA present around 30% of biodegradability, and these results are in agreement with other studies performed under similar conditions (Moura et al. 2012, 2011). A small increase of the biodegradability was detected for nanocomposites containing C 30 B and C 15 A . A possible explanation is that the presence of clays increases the hydrophilicity of a polymer matrix, allowing an easier permeability of water and activating the hydrolytic degradation process. Moreover, the lower

molecular weight of PLA nanocomposites when compared with pristine polymer could also increase polymer hydrolysis. The improvement of nanocomposite biodegradation is not visible in the first week because the water diffusion rate into the polymer can be lower due to the clay platelets like morphology, which maximizes the permeate path length through the nanocomposites (Fukushima et al. 2009a).

The higher biodegradability of the nanocomposites with C30B can be associated to the presence of terminal hydroxylated edge groups of this clay. The results obtained for nanocomposites with C15A may be explained by the presence of clay aggregates (Bikiaris 2013).

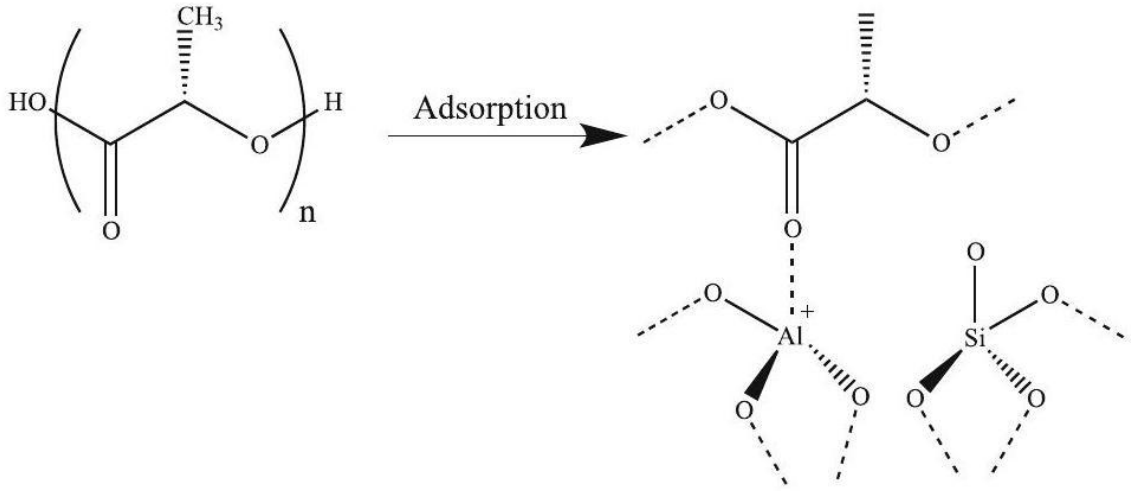

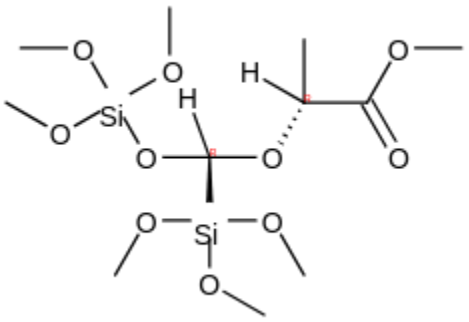

Polymer Chain Cleavage

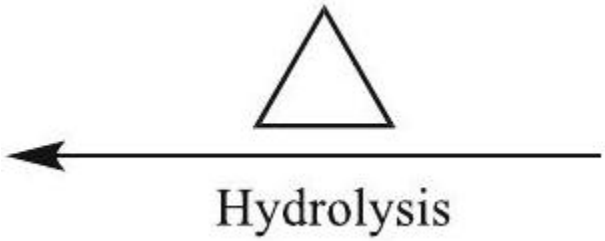

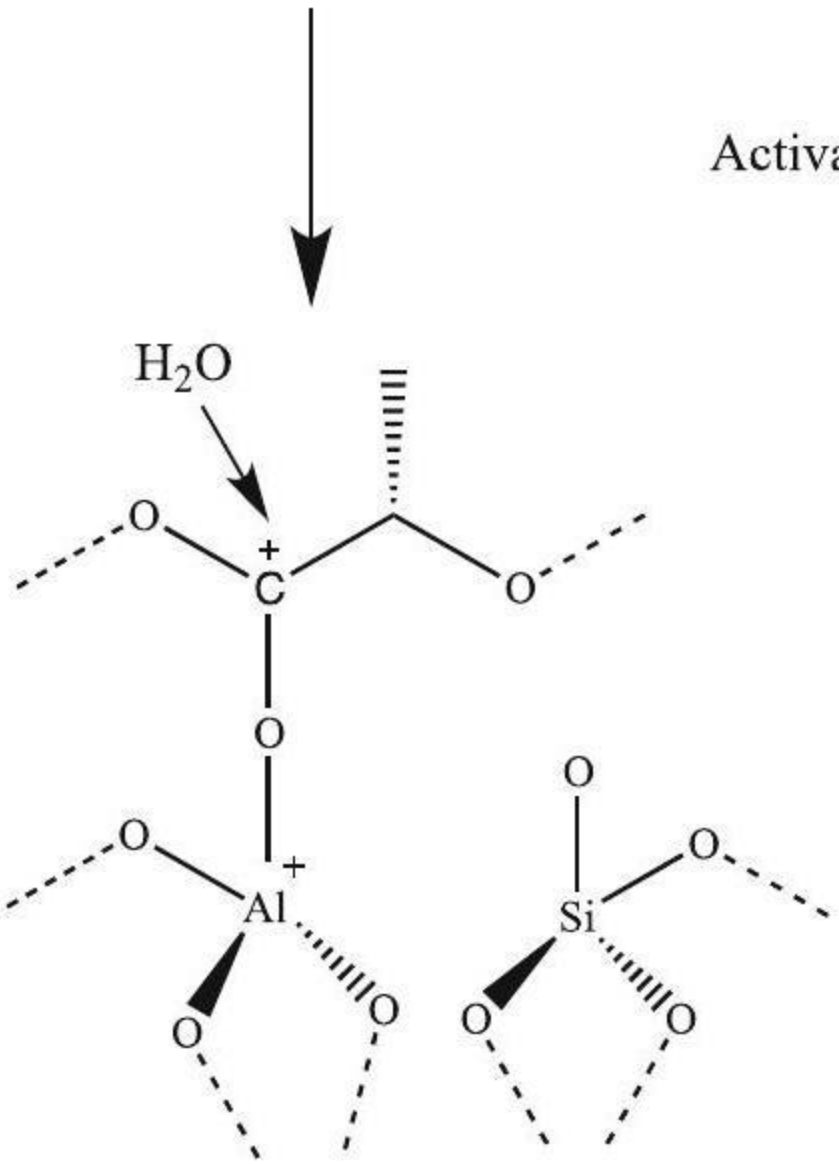
Activati
H2O
O
C
O
O
O
Al
O
O
O
O
Si
O
O
O

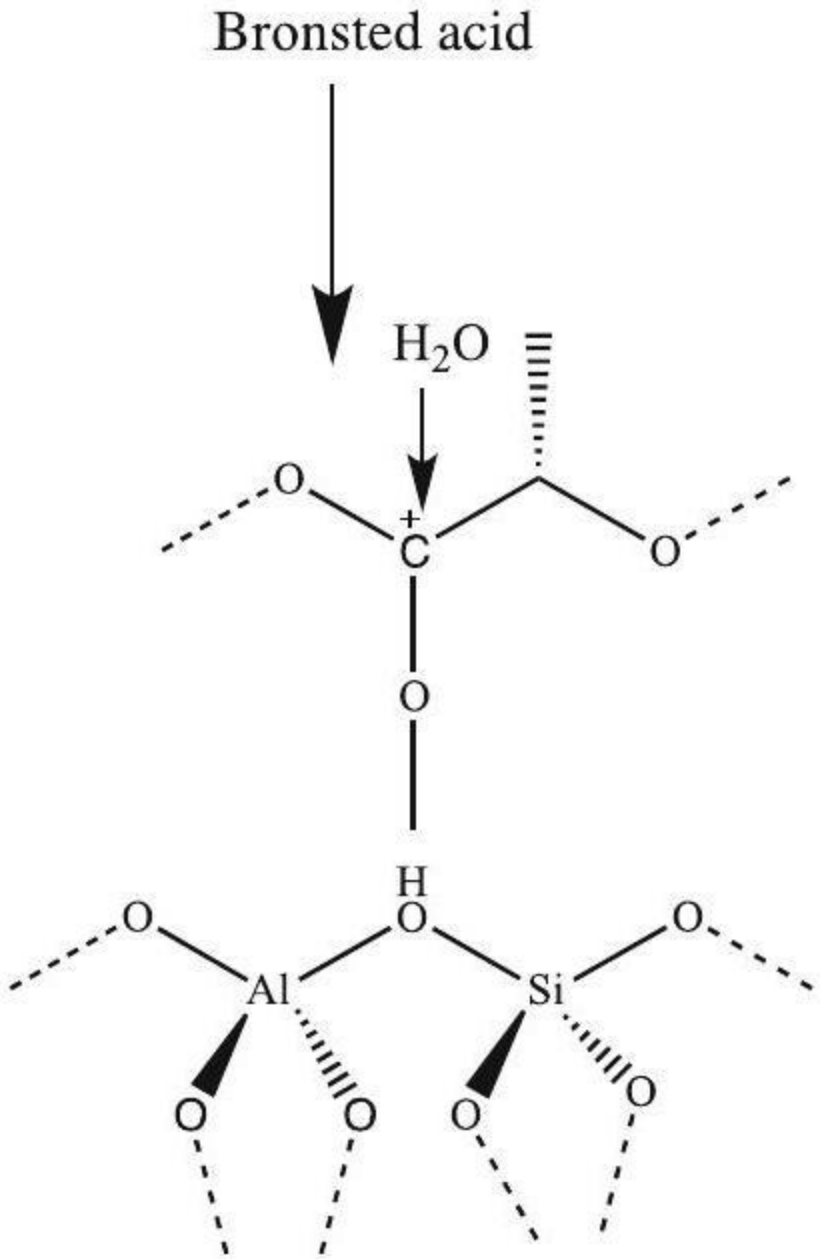

Fig. 6 Thermal degradation mechanism propose by (Okamoto et al. 2005)

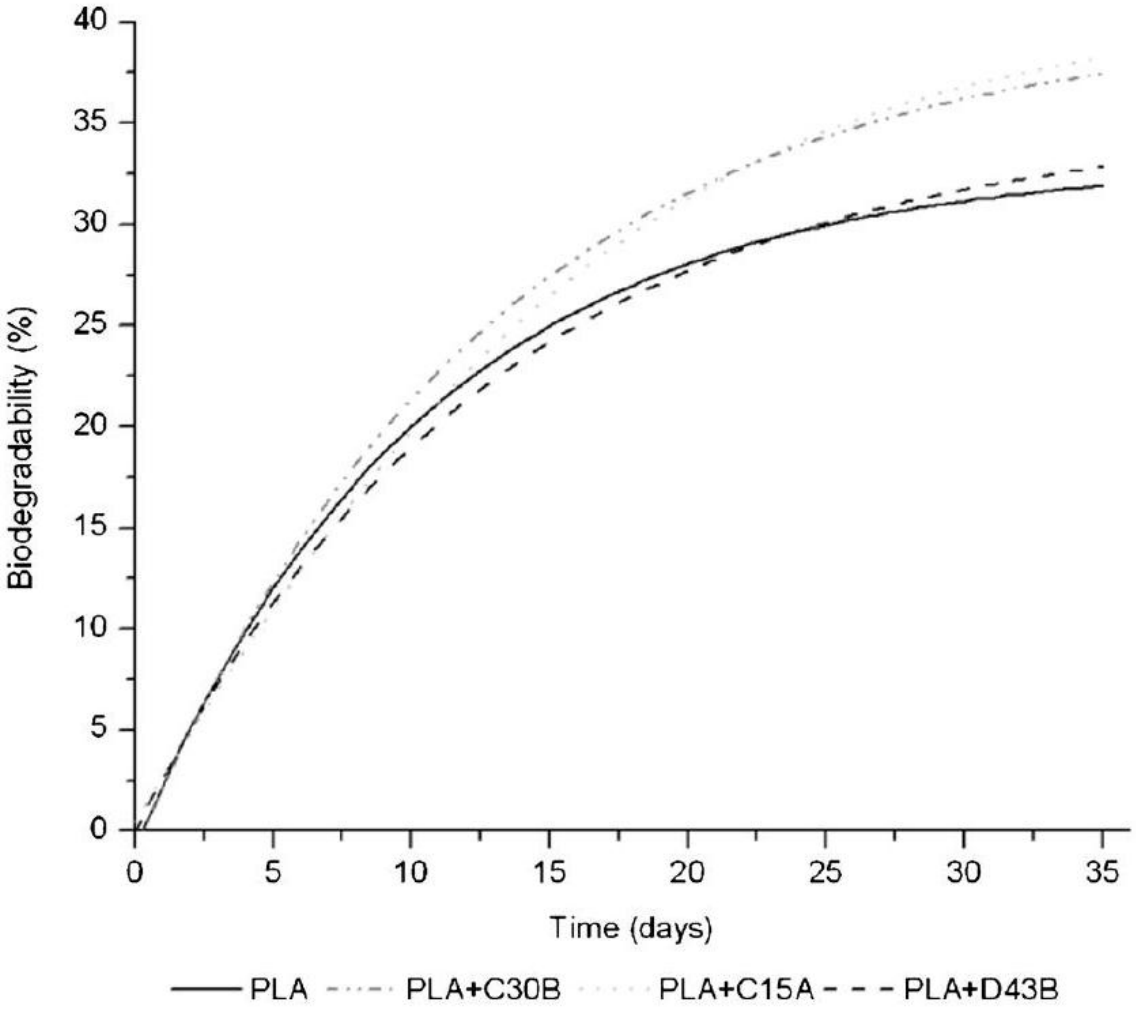

Fig. 7 Percentage of biodegradation of the PLA and PLA nanocomposites, without nitrification inhibitor, according to ISO 14851 (1999)

In general, the degradation of PLA in compost is a complex process involving four main phenomena: (1) water adsorption, (2) ester bond cleavage and formation of oligomer fragments, (3) solubilization of oligomer fragments, and finally (4) diffusion of soluble oligomers by bacteria in terms of CO_2 evolution. Any factor that increases the hydrolysis tendency of the PLA matrix will ultimately control the degradation of PLA (Sinha Ray et al. 2003a).

Figure **8** presents real pictures of PLA and nanocomposites after 6 weeks in compost. It is clear that most of the PLA and nanocomposites with D43B samples that were recovered are still intact. The surface whitening, visible in some parts of PLA samples and in all samples with D43B, can be a signal that the process of hydrolytic degradation of the polymer matrix has started, thus inducing a change in the refraction index of the sample as a consequence of water absorption and/ or presence of products formed by the hydrolytic process (Fukushima et al. 2009a). All samples containing C30B and C15A were recovered in small pieces evidencing high degradation level.

The weight of initial and samples collected along time was measured and the evolution (residual weight in percentage) is depicted in Fig. 9. After 6 weeks in compost, PLA and nanocomposites with D 43 B present a small decrease of weight, while the presence of C30B and C15A seemed to enhance the PLA degradation, as higher weight loss was observed. These results show the same trend of samples degradation as the ones obtained by biochemical oxygen demand in a closed respirometer.

To evaluate the extent of degradation of PLA and nanocomposites, the initial and collected samples were analysed by GPC (Fig. 10). A clear change in molecular weight can be observed after 6 weeks in compost at 40°C. The lower molecular weight of PLA nanocomposites (C15A and D43B) when compared with PLA can be explained by the temperature and shear during mixing of PLA and clays, resulting in the hydrolysis of PLA (Nieddu et al. 2009). PLA

Fig. 8 Real pictures of PLA and nanocomposites recovered from compost after 6 weeks

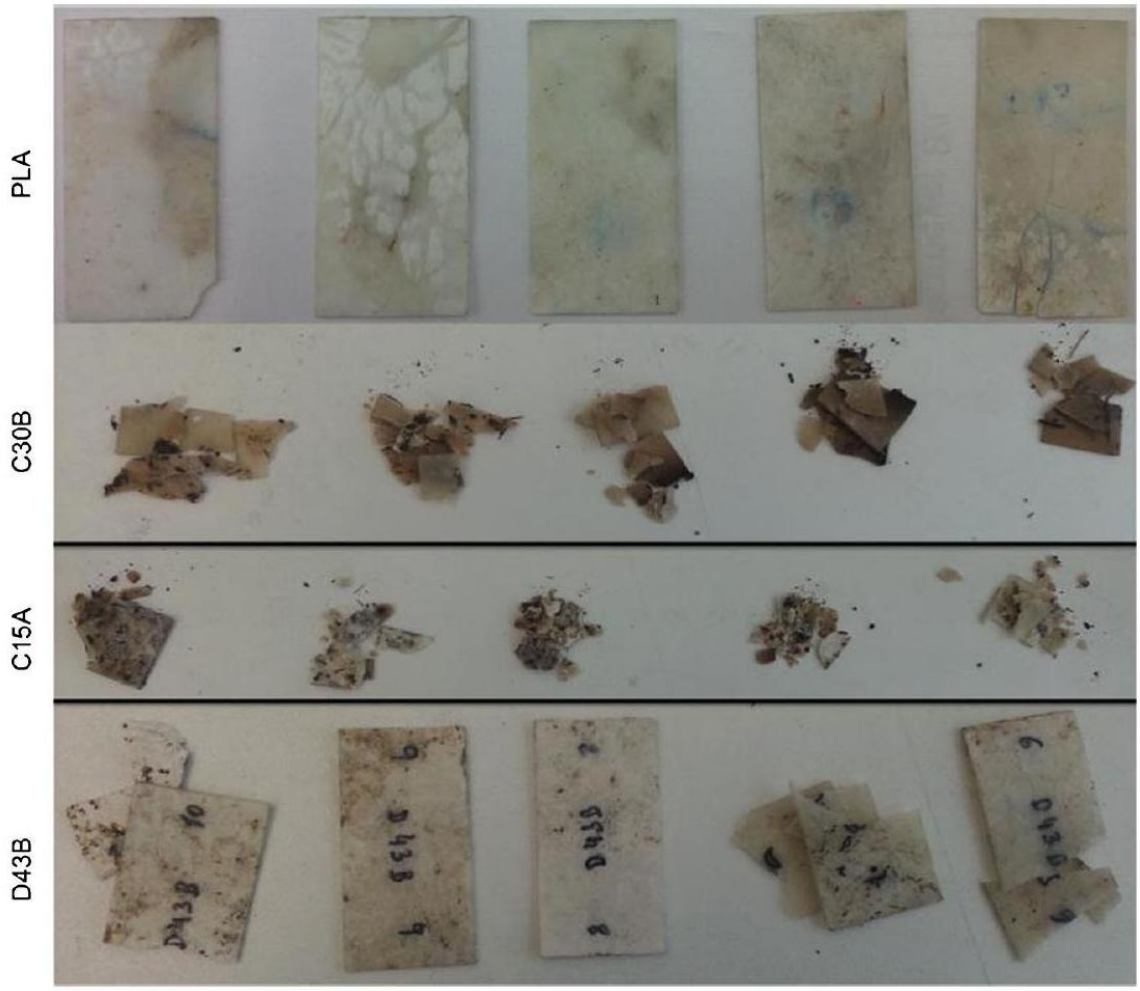

Fig. 9 Residual weight of PLA and nanocomposites after 3 and 6 weeks of degradation in compost

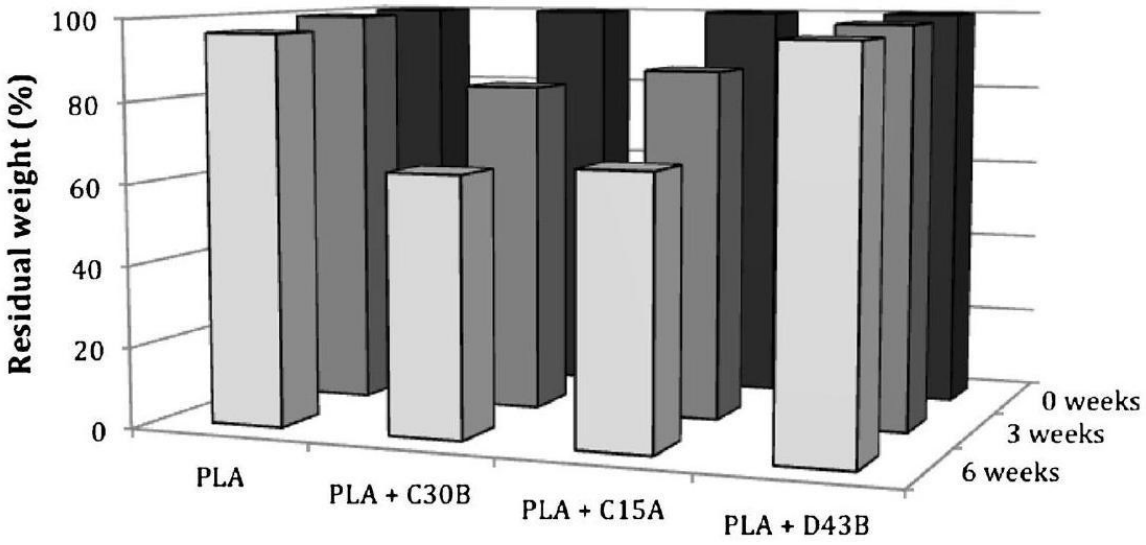

and nanocomposites curves show a shift to lower molecular weight (higher retention time), which indicates that chain scission of the long molecules occurred and smaller ones were formed. Moreover, the unimodal initial distribution became bi-, or in the case of D 43 B , tri-modal, indicating the presence of different types of molecules with lower molecular weights. In agreement with the degree of degradation visible in the pictures of Fig. 8, nanocomposites with C 30 B and C 15 A present higher reduction in molecular weight. Moreover, it is clear that the long molecules disappear due to intensive chain scission, and a peak due to smaller molecules appears. In the case of nanocomposite containing C 30 B , it can be due to the presence of hydroxyl groups; the fine dispersion of the organoclay in PLA may play a catalytic role on hydrolysis of the ester groups of the PLA matrix.

The results of Fig. 10 indicate that the reaction mechanism is not affected by the presence of nanoclay. Similar results were observed during UV exposure.

For PLA, GPC characterization was performed for samples collected after 3 and 6 weeks in compost. Since the PLA samples showed white and transparent zones, the analysis

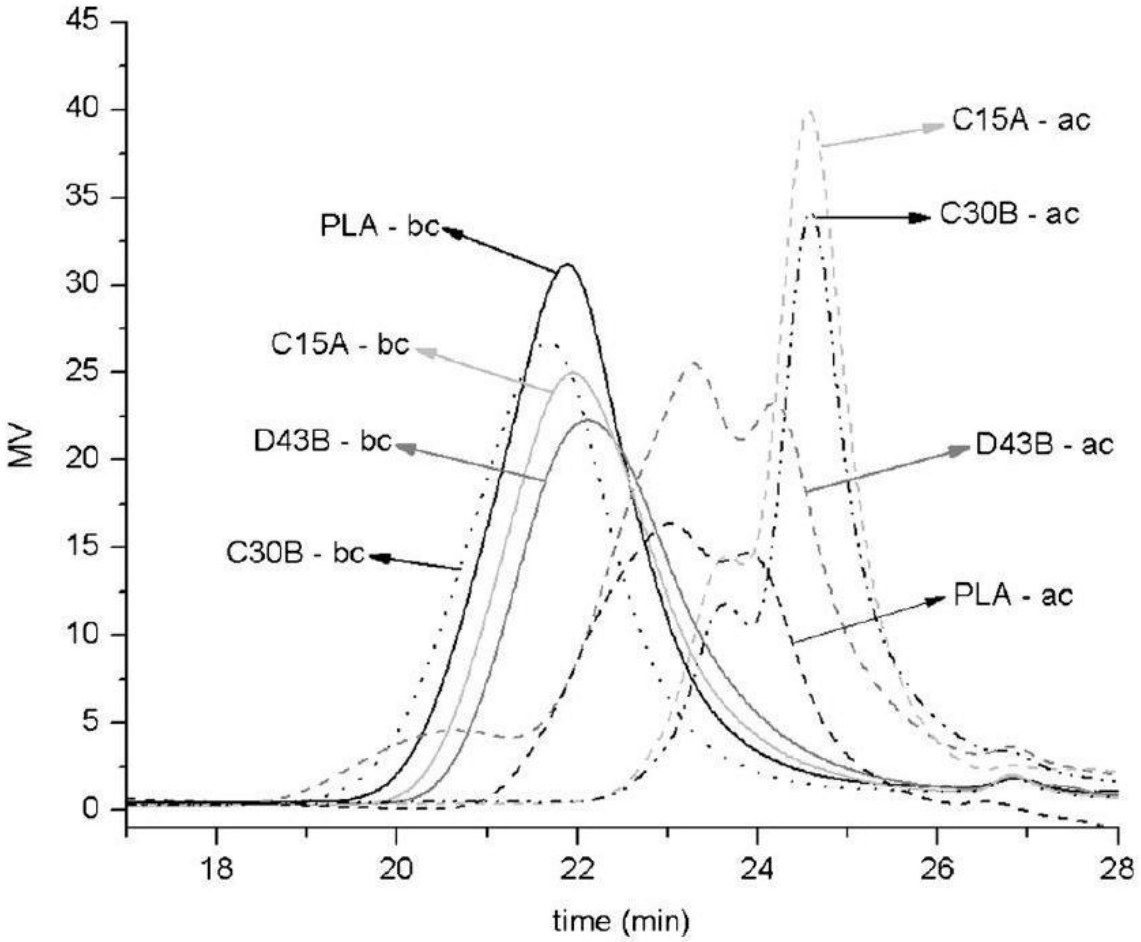

Fig. 10 GPC curves of PLA and nanocomposites before (*bc*) and after (ac) 6 weeks of degradation in compost

was made in both samples areas. The results depicted in Fig. 11 demonstrate the evolution of molecular weight along the time and in the different parts of the sample degraded in compost. As stated above, these results confirm that white zones correspond to smaller molecules, i.e., where the hydrolytic degradation was more intense. As shown before, the molecular weight decreases as the time increases, and the curves change from unimodal to bi-modal.

Concerning to the evolution of the mechanical properties of the samples collected from the compost, nanocomposites containing C30B and C15A were already removed as pieces. Even though PLA and PLA with D43B were intact, they broke when the tensile test started. Thus, a significant loss of mechanical properties occurred when the samples were placed in the compost, even after 3 weeks.

Conclusions

The degradability and biodegradability of PLA and its nanocomposites with C30B, C15A, and D43B were studied

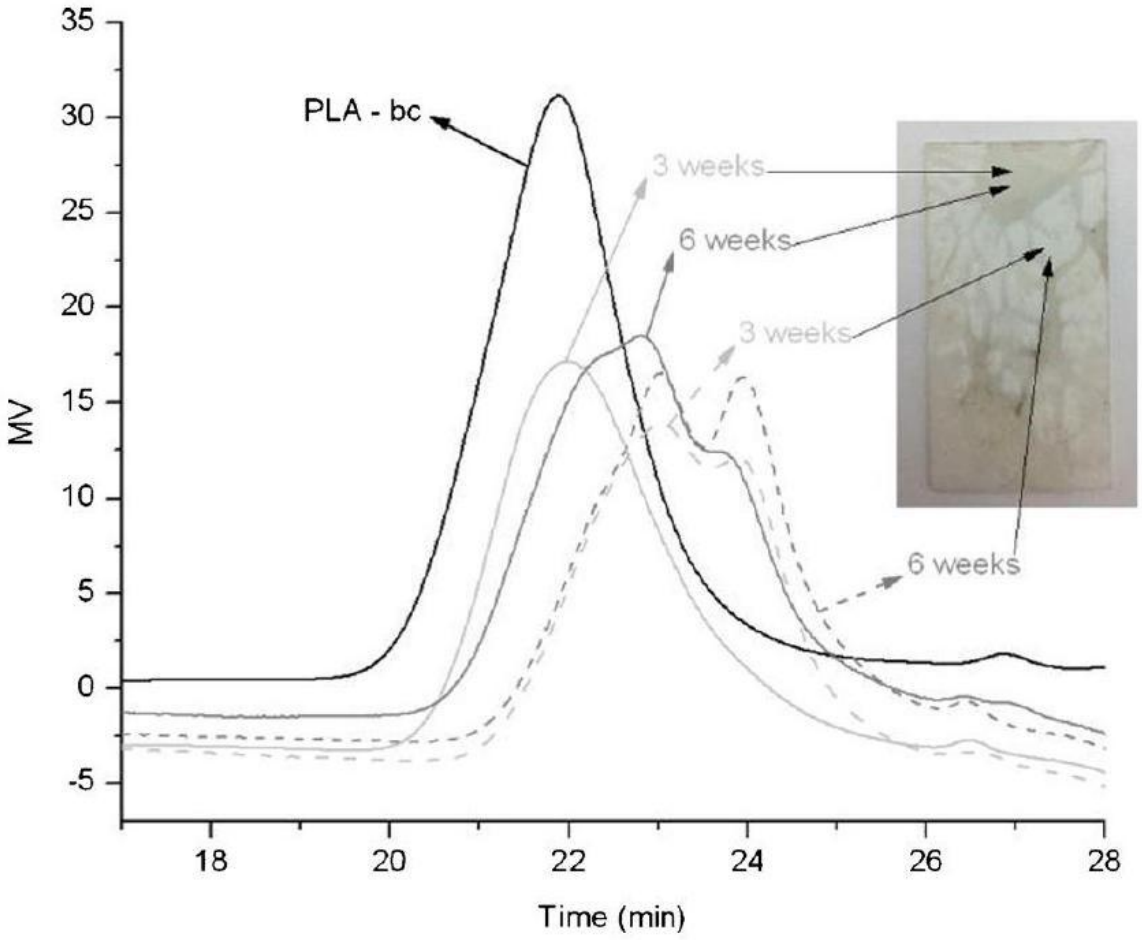

Fig. 11 GPC curves of PLA before (*bc*), and after 3 and 6 weeks of degradation in compost after the exposure to UV radiation, temperature, and microorganisms (solution and compost).

FTIR spectra and intrinsic viscosity measurements show that the nanoclay incorporation lead to an increase of thermal stability. The UV degradation was enhanced in the nanocomposites, but the degradation mechanism of PLA was not affected by the clays' presence.

The biological tests showed the same trend of biodegradation of the samples in solution and compost. Moreover, GPC results confirmed the chain scission occurred in all samples, but it was more intense for nanocomposites.

Acknowledgments The authors acknowledge the financial support given by FCT through the project PEst-C/CTM/LA0025/2011.

References

Araújo A, Botelho GL, Silva M, Machado AV (2013) UV stability of poly (lactic acid) nanocomposites. J Mat Sci Eng B 3(2):75-83
Belbachir S, Zaïri F, Ayoub G, Maschke U, Naït-Abdelaziz M, Gloaguen JM, Benguediab M, Lefebvre JM (2010) Modelling of photodegradation effect on elastic-viscoplastic

behaviour of amorphous polylactic acid films. J Mech Phys Solids 58(2):241255. doi:10.1016/j.jmps.2009.10.003

Bikiaris D (2011) Can nanoparticles really enhance thermal stability of polymers? Part II: an overview on thermal decomposition of polycondensation polymers. Thermochim Acta 523(1-2):25-45. doi:10.1016/j.tca.2011.06.012
Bikiaris DN (2013) Nanocomposites of aliphatic polyesters: an overview of the effect of different nanofillers on enzymatic hydrolysis and biodegradation of polyesters. Polymer Degradation and Stability 98: 1908-1928
Bocchini S, Fukushima K, Blasio AD, Fina A, Frache A, Geobaldo F (2010) Polylactic acid and polylactic acid-based nanocomposite photooxidation. Biomacromolecules 11(11):2919-1926
Bordes P, Pollet E, Averous L (2009) Nano-biocomposites: biodegradable polyester/nanoclay systems. Prog Polym Sci 34(2):125-155. doi:10. 1016/j.progpolymsci.2008.10.002
Carrasco F, Pagès P, Gámez-Pérez J, Santana OO, Maspoch ML (2010) Processing of poly(lactic acid): characterization of chemical structure, thermal stability and mechanical properties. Polym Degrad Stab 95(2): 116-125. doi:10.1016/j.polymdegradstab. 2009.11.045
Copinet A, Bertrand C, Longieras A, Coma V, Couturier Y (2003) Photodegradation and biodegradation study of a starch and poly (lactic acid) coextruded material. J Polym Environ 11(4):169-179
Dadbin S, Naimian F, Akhavan A (2011) Poly (lactic acid)/layered silicate nanocomposite films: morphology, mechanical properties, and effects of γ-radiation. J Appl Polym Sci 122(1):142-149
Frache A, Bocchini S (2013) Comparative study of filler influence on polylactide photooxidation. eXPRESS Polymer Letters 7:431-442
Fukushima K, Abbate C, Tabuani D, Gennari M, Camino G (2009a) Biodegradation of poly(lactic acid) and its nanocomposites. Polym Degrad Stab 94(10):1646-1655. doi:10.1016/j.polymdegradstab. 2009.07.001

Fukushima K, Tabuani D, Camino G (2009b) Nanocomposites of PLA and PCL based on montmorillonite and sepiolite. Mater Sci Eng C 29(4):1433-1441. doi:10.1016/j.msec.2008.11.005
Fukushima K, Tabuani D, Arena M, Gennari M, Camino G (2013) Effect of clay type and loading on thermal, mechanical properties and biodegradation of poly (lactic acid) nanocomposites. React Funct Polym 73(3):540-549
Gardette M, Thérias S, Gardette J-L, Murariu M, Dubois P (2011) Photooxidation of polylactide/calcium sulphate composites. Polym Degrad Stab 96(4):616-623. doi:10.1016/j.polymdegradstab. 2010. 12.023

Ikada E (1997) Photo-and bio-degradable polyesters. Photodegradation behaviors of aliphatic polyesters. J Photopolym Sci Technol 10(2): 265-270
ISO-4892-2 (2006) Plastics-methods of exposure to laboratory light sources-part 2: xenon-arc lamps
ISO-14851 (1999 (withdrawn 2005)) Determination of the ultimate aerobic biodegradability of plastic materials in an aqueous medium-method by measuring the oxygen demand in a closed respirometer
Kister G, Cassanas G, Vert M (1998) Effects of morphology, conformation and configuration on the IR and Raman spectra of various poly (lactic acid)s. Polymer 39(2):267-273
Lee S-R, Park H-M, Lim H, Kang T, Li X, Cho W-J, Ha C-S (2002) Microstructure, tensile

properties, and biodegradability of aliphatic polyester/clay nanocomposites. Polymer 43(8):2495-2500
Lewitus D, McCarthy S, Ophir A, Kenig S (2006) The effect of nanoclays on the properties of PLLA-modified polymers part 1: mechanical and thermal properties. J Polym Environ 14(2):171-177
Li B, Dong F-X, Wang X-L, Yang J, Wang D-Y, Wang Y-Z (2009) Organically modified rectorite toughened poly (lactic acid): nanostructures, crystallization and mechanical properties. Eur Polym J 45(11):2996-3003
Liu X, Zou Y, Li W, Cao G, Chen W (2006) Kinetics of thermo-oxidative and thermal degradation of poly(D, L-lactide) (PDLLA) at processing temperature. Polym Degrad Stab 91(12):3259-3265. doi:10.1016/j.polymdegradstab.2006.07.004
Madhavan Nampoothiri K, Nair NR, John RP (2010) An overview of the recent developments in polylactide (PLA) research. Bioresour Technol 101(22):8493-8501. doi:10.1016/j.biortech.2010.05.092
Massardier-Nageotte V, Pestre C, Cruard-Pradet T, Bayard R (2006) Aerobic and anaerobic biodegradability of polymer films and physico-chemical characterization. Polym Degrad Stab 91(3):620-627
Meaurio E, Lopez-Rodriguez N, Sarasua J (2006) Infrared spectrum of poly (L-lactide): application to crystallinity studies. Macromolecules 39(26):9291-9301
Moura I, Machado A, Duarte F, Nogueira R (2011) Biodegradability assessment of aliphatic polyesters-based blends using standard methods. J Appl Polym Sci 119(6):3338-3346
Moura I, Nogueira R, Bounor-Legare V, Machado A (2012) Synthesis of EVA-g-PLA copolymers using transesterification reactions. Mater Chem Phys 134(1):103-110
Nieddu E, Mazzucco L, Gentile P, Benko T, Balbo V, Mandrile R, Ciardelli G (2009) Preparation and biodegradation of clay composites of PLA. React Funct Polym 69(6):371-379. doi:10. 1016/j.reactfunctpolym.2009.03.002
Okamoto K, Toshima K, Matsumura S (2005) Degradation of poly(lactic acid) into repolymerizable oligomer using montmorillonite K10 for chemical recycling. Macromol Biosci 5(9):813-820. doi:10.1002/ mabi. 200500086
Pagga U (1997) Testing biodegradability with standardized methods. Chemosphere 35(12):2953-2972
Pandey JK, Raghunatha Reddy K, Pratheep Kumar A, Singh RP (2005) An overview on the degradability of polymer nanocomposites. Polym Degrad Stab 88(2):234-250. doi:10.1016/ j.polymdegradstab.2004.09.013

Petinakis E, Liu X, Yu L, Way C, Sangwan P, Dean K, Bateman S, Edward G (2010) Biodegradation and thermal decomposition of poly (lactic acid)-based materials reinforced by hydrophilic fillers. Polym Degrad Stab 95(9):1704-1707
Rhim J-W, Park H-M, Ha C-S (2013) Bio-nanocomposites for food packaging applications. Progress in Polymer Science 38:1389-1772

Sinha Ray S, Yamada K, Okamoto M, Fujimoto Y, Ogami A, Ueda K (2003a) New polylactide/layered silicate nanocomposites. 5. Designing of materials with desired properties. Polymer 44(21): 6633-6646
Sinha Ray S, Yamada K, Okamoto M, Ueda K (2003b) New polylactidelayered silicate nanocomposites. 2. Concurrent improvements of material properties, biodegradability and melt rheology. Polymer 44(3):857-866
Solarski S, Ferreira M, Devaux E (2008) Ageing of polylactide and polylactide nanocomposite filaments. Polym Degrad Stab 93(3): 707-713. doi:10.1016/j.polymdegradstab.2007.12.006
Therias S, Larché J-F, Bussière P-O, Gardette J-L, Murariu M, Dubois P (2012)

Photochemical behavior of polylactide/ZnO nanocomposite films. Biomacromolecules 13(10):3283-3291
Tokiwa Y, Calabia BP (2006) Biodegradability and biodegradation of poly (lactide). Appl Microbiol Biotechnol 72(2):244-251
Wu T-M, Wu C-Y (2006) Biodegradable poly(lactic acid)/chitosanmodified montmorillonite nanocomposites: preparation and characterization. Polym Degrad Stab 91(9):2198-2204. doi:10. 1016/j.polymdegradstab.2006.01.004

Wu X, Yuan J, Yu Y, Wang Y (2009) Preparation and characterization of polylactide/montmorillonite nanocomposites. J Wuhan Univ Technol-Mater Sci Ed 24(4):562-565
Zaidi L, Bruzaud S, Bourmaud A, Médéric P, Kaci M, Grohens Y (2010a) Relationship between structure and rheological, mechanical and thermal properties of polylactide/Cloisite 30 B nanocomposites. J Appl Polym Sci 116(3):1357-1365
Zaidi L, Kaci M, Bruzaud S, Bourmaud A, Grohens Y (2010b) Effect of natural weather on the structure and properties of polylactide/ Cloisite 30B nanocomposites. Polym Degrad Stab 95(9):17511758. doi:10.1016/j.polymdegradstab.2010.05.014

Zhou Q, Xanthos M (2009) Nanosize and microsize clay effects on the kinetics of the thermal degradation of polylactides. Polym Degrad Stab 94(3):327-338. doi:10.1016/j. polymdegradstab. 2008.12.009
Zhu H, Zhu Q, Li J, Tao K, Xue L, Yan Q (2011) Synergistic effect between expandable graphite and ammonium polyphosphate on flame retarded polylactide. Polym Degrad Stab 96(2):183-189. doi:10.1016/j.polymdegradstab.2010.11. 017